

We are IntechOpen, the world's leading publisher of Open Access books Built by scientists, for scientists

5,300

Open access books available

130,000

International authors and editors

155M

Downloads

Our authors are among the

154

Countries delivered to

TOP 1%

most cited scientists

12.2%

Contributors from top 500 universities



WEB OF SCIENCE™

Selection of our books indexed in the Book Citation Index
in Web of Science™ Core Collection (BKCI)

Interested in publishing with us?
Contact book.department@intechopen.com

Numbers displayed above are based on latest data collected.

For more information visit www.intechopen.com



Recent Advances in Applications of Ceramic Nanofibers

Nuray Kizildag

Abstract

Ceramic materials are well known for their hardness, inertness, superior mechanical and thermal properties, resistance against chemical erosion and corrosion. Ceramic nanofibers were first manufactured through a combination of electrospinning with sol-gel method in 2002. The electrospun ceramic nanofibers display unprecedented properties such as high surface area, length, thermo-mechanical properties, and hierarchically porous structure which make them candidates for a wide range of applications such as tissue engineering, sensors, water remediation, energy storage, electromagnetic shielding, thermal insulation materials, etc. This chapter focuses on the most recent advances in the applications of ceramic nanofibers.

Keywords: applications, Li-ion battery, catalysts, ceramic nanofibers, electromagnetic shielding, electrospinning, nanofiber, sensors, thermal insulation, tissue engineering, water remediation

1. Introduction

Nanofibers are 1D nanostructured materials with some distinctive characteristics, such as large surface areas, well-controlled composition, flexibility, tunable porosity, ease of surface functionalization, and high mechanical/thermal properties which make them suitable for a number of different applications such as energy harvesting and storage [1, 2], filtration [3, 4], sensors [5, 6], tissue engineering [7–9], wound healing [10, 11], drug delivery [12, 13], polymer reinforcement [14, 15], and so on.

The possibility of producing nanofibers from a wide range of materials, including polymers, metals and metal oxides, carbon-based, and composite nanomaterials forms the significant impact of nanofiber technology [16]. The development of ceramic nanofibers has attracted a significant interest over the recent years. Ceramic nanofibers (CNFs) have been developed by the application of different methods such as magnetron sputtering [17], solution blowing [18], laser spinning [19], chemical vapor deposition [20], template synthesis [21], phase separation [22], hydrothermal treatment [23], and electrospinning [24–26]. Various kinds of ceramic nanofibers classified roughly into two groups such as oxide nanofibers (SiO_2 , SnO_2 , TiO_2 , $\alpha\text{-Al}_2\text{O}_3$, WO_3 , BaTiO_3) and non-oxides (carbides (B_4C , SiC), borides, nitrides, silicides, sulfides) have been fabricated and are proven to be used in many different applications with high performance and efficiency.

2. Electrospinning of ceramic nanofibers

Electrospinning is the most used nanofiber production technique. It uses electrostatic forces to produce nanofibers. The electrospinning setup consists of a pump, high-voltage power supply, and a collector. The pump feeds the solution to the tip of the needle, the high-voltage power supply charges the solution, and the grounded collector collects the nanofibers. A jet occurs as the electrostatic force overcomes the surface tension of the solution droplet, undergoes bending and whipping instability during its flight in the electrical field between the tip of the needle and the collector. As the solvent evaporates, nanofibers accumulate on the collector in the nanoweb form. Electrospinning is a very simple and relatively inexpensive method used to fabricate ceramic nanofibers and it allows to control the morphology, average diameters, and compositions of the nanofibers (CNFs) [27–30].

Electrospinning enables the production of CNFs with very small diameters, high surface areas, extremely long length, and small pore size. The fabrication of CNFs by electrospinning is usually achieved in three main steps (**Figure 1**): (i) preparation of an electrospinning solution containing a polymer and sol-gel precursor; (ii) electrospinning of the solution to generate precursor NFs; and (iii) conversion of precursor NFs into the final CNFs by calcination, sintering, or chemical processes [31–36]. CNFs requires the presence of a polymer phase in the electrospinning solution as the ceramic phase on its own is not suitable for electrospinning. For successful electrospinning of CNFs, a suitable combination of ceramic precursor, polymer and solvent that can form a viscous homogeneous solution should be selected. Polyvinyl alcohol (PVA) [37], polyethylene oxide (PEO) [38], and polyvinyl pyrrolidone (PVP) [39] are widely used as the polymer phase in the electrospinning of CNFs.

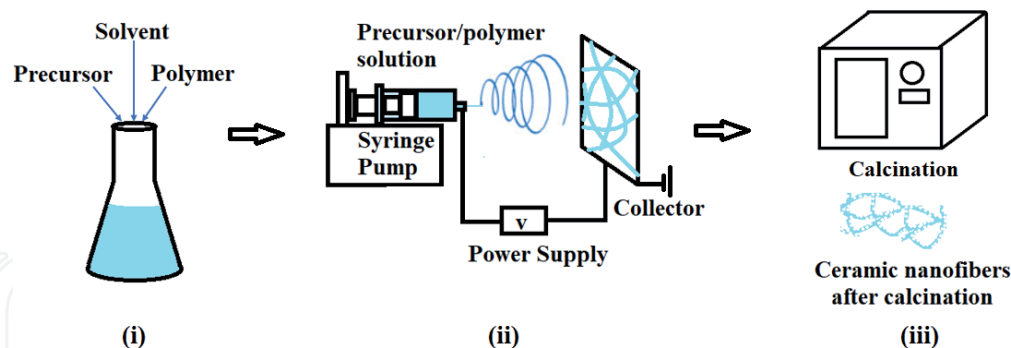


Figure 1. Schematic showing the preparation of ceramic nanofiber membranes.

3. Applications of ceramic nanofibers

The unique properties of CNFs such as high surface area, extraordinary length, low density, high porosity, and thermo-mechanical properties [40, 41] qualify them for many different applications. This chapter covers a review of their applications related to tissue engineering [35, 36, 42–47], sensors [32–34, 48, 49], water remediation [50–56], batteries [57–63], catalyst supports/catalysts [64–71], electromagnetic interference (EMI) shielding [72–79], and thermal insulation materials [26, 79–82], etc. A list of the recent studies about ceramic nanofibers by electrospinning method is presented in **Table 1**.

Ceramic nanofiber composition	Processes applied	Potential applications	Important results	Ref.
$\text{Ca}_{10}(\text{PO}_4)_6(\text{OH})_2$	electrospinning, calcination at 600°C	tissue engineering	uniform nanofibers with rough surface	[36]
$\text{Ca}_3(\text{PO}_4)_2$	electrospinning, calcination at 600°C	tissue engineering drug delivery	solid and micro-porous nanofibers	[35]
$\text{Ca}_{10}(\text{PO}_4)_6(\text{OH})_2$	electrospinning, heat treatment at 350°C	tissue engineering	structural analysis	[43]
TiO_2	electrospinning, calcination at 700°C	tissue engineering	supported osteoblast viability	[45]
TiO_2	electrospinning, calcination at 500°C bioceramic preparation using TiO_2 nanofibers as reinforcement	hard tissue engineering applications	bulk density, compressive strength and microhardness increased, porosity and water adsorption capacity decreased, bone-like apatite formation in simulated body fluid	[46]
BN reinforced gelatin	electrospinning, glutaraldehyde cross-linking	bone tissue engineering applications	nontoxic, biodegradable bioactive materials with enhanced mechanical properties	[47]
$8\text{CeO}_2 - 0.5\text{Y}_2\text{O}_3 - \text{ZrO}_2$	electrospinning, calcination at 1300°C	artificial muscle applications	Aligned nanofibers with shape-memory strain and repeatable shape memory actuation behavior	[42]
CeO_2	electrospinning, calcination at 1000°C	O_2 and CO monitoring	good morphological and structural stability in high temperature environment, sensitive, reversible, and reproducible response in real-time O_2 and CO monitoring	[32]
Ln FeO_3 (Ln = La, Nd, Sm)	electrospinning, calcination at 700°C	acetone sensor	lower optimum operating temperature (140°C) and good response	[49]
PrFeO_3	electrospinning, calcination at 600°C	acetone sensors	high response value, good selectivity, and good long-time stability at a low operating temperature of 180°C	[34]
silica, silica/PVP, silica/PMMA	electrospinning, drying at 50°C	optical gas sensor	flexible and porous nature, reliable and reproducible visual sensing performance	[48]
SmFeO_3	electrospinning, calcination at 700°C	ethylene glycol sensor	good response and distinct selectivity to ethylene glycol	[33]

Ceramic nanofiber composition	Processes applied	Potential applications	Important results	Ref.
α -Fe ₂ O ₃	electrospinning, calcination at 500°C	chromate removal in water treatment	adsorption capacity increased with decreasing diameter, outperformed the commercially available Fe ₂ O ₃ nanoparticles	[50]
CuO-ZnO composite	electrospinning, calcination at 500°C	water treatment and purification	high adsorption capacity, antibacterial activity	[53]
TiO ₂ Au coated TiO ₂	electrospinning, calcination at 800°C, Au coating	water treatment and purification	enhanced photoactivity	[52]
NiO nanofibers	electrospinning, calcination at 500°C	photocatalyst in water treatment	highly stable and ultrafine nanofibers with photocatalytic activity against congo red model dye	[83]
ZnO ZnO-SnO ₂ composite	electrospinning, calcination at 600°C	photocatalyst in water treatment	ZnO-SnO ₂ nanofibers showed higher photocatalytic activity than ZnO nanofibers, which was dependent on Sn/Zn molar ratio	[54]
ZnO/fly ash	electrospinning, calcination at 500°C	photocatalyst and adsorbent in water treatment	enhanced adsorption capacity and photocatalytic efficiency	[55]
TiO ₂ -coated YSZ/silica NF	electrospinning, calcination at 500°C	photocatalyst in water treatment	stable and reusable membranes with improved photocatalytic degradation efficiency and self-cleaning functionality	[51]
SiO ₂ nanofibers/Al ₂ O ₃ nanoparticles	electrospinning, calcination at 500, 600, 700, and 800°C	separator for LIBs	Nanofiber membranes with smooth surface, polymer-free composition, high porosity (79%), high electrolyte uptake (876%), and excellent thermal stability Full cell with reversible discharge capacity of 165 mAh g ⁻¹ after 100 cycles at a current density of 50 mA g ⁻¹	[57]
ZrO ₂	electrospinning, calcination at 800°C	separator for LIBs and NaIBs	remarkable mechanical flexibility, ample porosity, excellent electrolyte wettability and infiltration, outstanding heat and flame-resistance, and high electrochemical inertness, in lithium or sodium batteries, higher current densities, longer cycling lives	[59]

Ceramic nanofiber composition	Processes applied	Potential applications	Important results	Ref.
CuO nanofibers	electrospinning, calcination at 600°C	anode for LIBs	specific capacity of 310 mAh g ⁻¹ at 1C rate for 100 cycles and stabilized capacity of about 120 mAh g ⁻¹ at 5C rate for 1000cycles	[60]
Co ₃ O ₄ @rGO nanofiber	electrospinning, calcination at 600°C, rGO coating	anode for LIBs	efficient stress relaxation and fast Li ⁺ ions and electron transport during discharge/charge cycling, in a half cell, displayed high Coulombic efficiency, enhanced cyclic stability, and high-rate capability (~900mAh/g at 1A/g, and ~ 600mAh/g at 5A/g) in half cell	[61]
3D SiO ₂ nanofibers in polyethylene oxide–lithium (bis trifluoromethyl) sulfate–succinonitrile (PLS)	impregnating nanofiber membranes by PLS	solid polymer electrolyte for batteries	specific capacity of 167.9 mAh g ⁻¹ , suffered only 3.28% capacity degradation after 100 cycles, high safety at elevated temperatures by automatic shut down	[58]
aluminum-doped Li _{0.33} La _{0.557} TiO ₃ (LLTO) nanofiber network in a polyvinylidene fluoride-hexafluoropropylene (PVDF-HFP)	electrospinning, calcination at 900°C, impregnation	solid polymer electrolyte for batteries	improved ionic conductivity and electrochemical cyclic stability, a full cell with excellent cycling performance and rate capability	[62]
γ-Al ₂ O ₃	electrospinning, calcination	catalyst supports	sinter-resistant performance up to 500°C, higher reaction rates in the catalytic reduction of p-nitrophenol, compared to free nanocrystals	[68]
MgTiO ₃	electrospinning, calcination at 600°C	photocatalyst for H ₂ generation	enhanced efficiency and stability in photocatalytic H ₂ generation under ultraviolet light	[71]
CuO-NiO composite	electrospinning, calcination at 600°C	catalyst for hydrazine oxidation	Ni content dependent electro-catalytic activity when used for hydrazine oxidation in alkaline media	[69]
CeO ₂ /Al ₂ O ₃	electrospinning, calcination at 500°C	catalyst supports	homogenous elemental distribution, displayed good sinter-resistant performance and exhibited 13-times great catalytic activity than that of Pt@Al ₂ O ₃ catalyst towards the hydrogenation of p-nitrophenol	[70]

Ceramic nanofiber composition	Processes applied	Potential applications	Important results	Ref.
TiO ₂ ZrO ₂	electrospinning, calcination at 510, 550, and 800°C	catalytic system for Suzuki cross-coupling reactions	calcination temperature dependent phase, Pd on anatase TiO ₂ could be used to catalyze the Suzuki coupling reactions and operated in a continuous flow fashion, nitric acid treatment provided reactivation	[67]
SiC	electrospinning, calcination at 1350°C	EMI shielding	flexible, hydrophobic, corrosion resistant, and thermally stable nanofibers with excellent EMI shielding properties with an effective absorption bandwidth of 4–18 GHz	[75]
SiC-Si ₃ N ₄ /graphite	electrospinning, calcination at 800, 1300, 1400, and 1500°C	EMI shielding	nanofibers annealed at 1300°C in Ar showed a RL _{min} of –57.8 dB at 14.6 GHz with EAB of 5.5 GHz, nanofibers annealed at 1300°C in N ₂ exhibited a RL _{min} of –32.3 dB with EAB of 6.4 GHz over the range of 11.3–17.7 GHz	[76]
SiC/ZrC/SiZrOC nanofibers	electrospinning, calcination at 1400 and 1500°C	EMI shielding	reasonable electrical conductivity microwave-absorbing capability RL _{min} of about –40.38 dB at 14.1 GHz, antioxidant properties at 600°C	[72]
SiC/C	electrospinning, calcination at 1400°C	EMI shielding	lightweight and high EMI shielding efficiency, an ultrathin paraffin matrix with 30 wt.% SiC/C nanofibers exhibited superior EM wave absorption performance (RL < –10 dB) over the range of 12.6 and 16.7 GHz	[73]
ZrC/SiC	electrospinning, calcination at 1300-1500°C	EMI shielding	Flexible, lightweight nanofiber mats, 3-layer ZrC/SiC nanofiber mats with a thickness of 1.8 mm showed EMI shielding effectiveness (SET) of 18.9 dB, further improved to 20.1 dB at 600°C	[74]
SiO ₂	electrospinning, calcination at 600, 800, 1000, and 1200°C	thermal insulation materials	ultra-softness, enhanced tensile strength, ultra-low thermal conductivity of 0.0058 W m ⁻¹ K ⁻¹	[77]
mullite	electrospinning, calcination between 900 and 1500°C	thermal insulation materials	diphasic nanofibers with average diameter of 216 ± 40 nm	[79]
SiO ₂ /aluminoborosilicate nanofibrous aerogels	electrospinning, calcination at 900°C	thermal insulation materials	flyweight densities of >0.15 mg cm ⁻³ , zero Poisson's ratio, rapid recovery from 80% strain, and temperature-invariant superelasticity up to 1100°C, robust fire resistance and thermal insulation performance	[78]

Ceramic nanofiber composition	Processes applied	Potential applications	Important results	Ref.
SiO ₂ /SiO ₂ nanofibrous aerogels	electrospinning, calcination at 900°C	thermal insulation materials	ultralow density of ~0.2 mg cm ⁻³ , ultralow thermal conductivity (23.27 mW m ⁻¹ K ⁻¹), negative Poisson's ratio, temperature-invariant superelasticity from -196 to 1100°C, and editable shapes on a large scale	[81]
SiZrOC	electrospinning, calcination at 800°C	thermal insulation materials	high-temperature stability (~1200°C in Ar) and low thermal conductivity (~0.1392 W m ⁻¹ K ⁻¹ at 1000°C in N ₂)	[26]
ZrO ₂ -Al ₂ O ₃ /Al(H ₂ PO ₄) ₃ nanofibrous aerogels	electrospinning, calcination at 800°C	thermal insulation materials	ultra-strong, superelastic, and high temperature resistant, high fatigue resistance, thermal insulation performance with low thermal conductivity (0.0322 W m ⁻¹ K ⁻¹)	[82]
yttria-stabilized zirconia mixed silica (YSZ/SiO ₂)	electrospinning, calcination at 800-1300°C	thermal insulation materials	enhanced use temperature and mechanical properties by stabilization, good thermal insulation performance and hydrophobic property	[80]
TiO ₂ nanofibers AgNP coating	electrospinning, calcination at 500°C, coating by impregnation	separation of nuclear waste and recycling of nuclear fuels	high porosity, permeability, loading capacity, stability in extreme conditions	[84]
ZnTiO ₃	electrospinning, calcination at 300-700°C	detoxification of chemical warfare agents	satisfactory reactivity against chemical warfare simulants	[85]
TiO ₂	electrospinning, calcination at 800°C	reinforcement in Mg composite	increased compressive strength	[86]
TiO ₂	electrospinning, calcination at 450°C	capacitive pressure sensor	high sensitivity (≈4.4 k Pa ⁻¹), fast response speed (<16 ms), ultralow limit of detection (<0.8 Pa), low fatigue over 50000 loading/unloading cycles, high temperature stability	[87]

Table 1.
Ceramic nanofibers by electrospinning method and their applications.

3.1 Tissue engineering applications

Tissue engineering scaffolds are often made of biodegradable polymeric materials. The biodegradable polymeric scaffolds are not widely used in regeneration of load-bearing bones due to their limited mechanical strength. There have been many efforts invested to enhance the mechanical properties of the scaffolds, i.e., CNFs, reinforced by hydroxyapatite (HA), have provided mechanical support and osteoconductivity to the growing cells in bone regeneration.

Wu et al. [36] electrospun a precursor mixture of $\text{Ca}(\text{NO}_3)_2 \cdot 4\text{H}_2\text{O}$ and $(\text{C}_2\text{H}_5\text{O})_3\text{PO}$ with a polymer additive, then applied thermal treatment at 600°C for 1 h and prepared HA ($\text{Ca}_{10}(\text{PO}_4)_6(\text{OH})_2$) fibers. The pure fibers obtained were 10–30 μm in diameter and up to 10 mm in length. The HA grain size was $\sim 1 \mu\text{m}$ [36]. Kim and Kim produced HA nanofibers and also their fluoridated forms for dental restoration applications to stimulate bone cell responses and provide protection against the formation of dental caries [44]. Xiaoshu and Shivkumar [35] electrospun nanofibers from polyvinyl alcohol (PVA) solution containing calcium phosphate-based sol and then calcined them at 600°C for 6 h to obtain an inorganic, fibrous network, which was suggested for use in the tissue engineering and drug delivery [35]. Franco et al. used phosphorus pentoxide (P_2O_5) and calcium nitrate tetrahydrate ($\text{Ca}(\text{NO}_3)_2 \cdot 4\text{H}_2\text{O}$) as precursors of phosphorus and calcium and polyvinylpyrrolidone (PVP) as the polymer to electrospin CNFs [43]. Wang et al. [45] electrospun pure titanium dioxide (TiO_2) nanofiber meshes with different surface microroughness and nanofiber diameters and investigated the osteoblast differentiation on these meshes by analyzing the cell number, differentiation markers and local factor production for MG63 cells seeded on TiO_2 meshes. Cells with similar morphology were observed to grow throughout the entire surfaces. While the cell number was found to be sensitive to surface microroughness, the cell differentiation and local factor production were observed to be regulated by both surface roughness and nanofiber diameter. These results indicated that the TiO_2 nanofiber meshes could be used to create an osteogenic environment without using exogenous factors [45]. Aly et al. [46] developed wollastonite glass ceramic composites reinforced by electrospun TiO_2 nanofibers for use in hard tissue engineering applications. The composite material exhibited greater densification and better mechanical characteristics in comparison to pure wollastonite. The composites having 0, 10, 20 and 30 wt.% metal oxide nanofibers were sintered at 900, 1100 and 1250°C . While the compressive strength, bulk density, and microhardness increased, the water adsorption capacity and porosity decreased with the increase in the TiO_2 nanofiber content. When the wollastonite and wollastonite/ TiO_2 nanofibers were soaked in simulated body fluid, bone-like apatite was formed on their surface. The characteristics of wollastonite were improved with incorporation of TiO_2 nanofibers while its in-vitro bioactivity was preserved. The developed composite was suggested for use as a bone substitute in high load bearing sites [46]. Nagarajan et al. [47] produced boron nitride-reinforced gelatin nanofibers as a new class of two-dimensional biocompatible nanomaterials, showing enhanced mechanical properties, stability to the glutaraldehyde cross-linking, high bioactivity in forming bone-like HA, and biodegradability. Depending on the analysis of osteoblast gene expression and the measurement of alkaline phosphatase activity, they were proven to be suitable for bone tissue engineering applications [47].

Apart from the use of CNFs in bone tissue engineering applications, Du et al. [42] recently fabricated highly aligned, zirconia-based, shape memory nanofiber yarns and springs by electrospinning for artificial muscle applications at elevated temperatures. The nanofiber yarns displayed a recoverable strain of up to $\sim 5\%$ and short recovery time (0.16 s) at actuation temperatures of $328\text{--}388^\circ\text{C}$. When heated

by a Bunsen burner, the shape memory ceramic springs could lift up to 87 times their own weight with a stroke of ~ 3.9 mm. The ceramic yarns/springs exhibited an output stress of 14.5–22.6 MPa, a work density of ~ 15 –20 kJ m⁻³, and a tensile strength of ~ 100 –200 MPa, which were much higher than those of human muscles and some other polymer-based artificial muscles [42].

3.2 Gas sensors

Sensors, which are used to monitor and quantify volatiles related to environmental monitoring, analyze food quality, and diagnose illnesses, have attracted great interest in the recent years. Sensors designed are required to display high selectivity, low power consumption, fast response/recovery rate, low detection limit and a low humidity dependence [31].

The ceramic nanofibers have been extensively studied for gas sensing applications due to their advantages such as good directional carrier transport, high surface energy, large surface-to-volume ratio, high chemical stability, great sensing performance. Ceramics are inherently resistant to aggressive physical and corrosive chemical circumstances and they offer significantly minimized hysteresis with increased relaxation time, which improves the stability, performance, and response time of pressure sensors [87]. Many researchers showed the applicability of electrospun ceramic nanofibers in gas sensing applications for detection of many different gases such as acetone [34, 49, 88–97], ethanol [98–101], formaldehyde [102], ammonia [103–107], hydrogen sulfide [108], nitrogen dioxide [109–111], acetic acid [112], carbon monoxide [113, 114], hydrogen [115], and toluene [116]. The sensing properties of metal oxides depend on their shape, size, size distribution, surface area, structure, phase, the grain size, crystallinity, the presence of crystal lattice defects, the type of the charge carriers, and the oxidizing or reducing nature of the target gas [31, 117–120]. Besides, the composition of the sensor is another important factor. The most effective methods for improving response time and sensitivity are (i) doping with different metals such as Ce, Cu, Pr, La, Pd, Mn [91, 94, 106, 112, 114, 121], (ii) formation of composites by coupling of two or more oxide metals [118, 119, 122–124], and (iii) addition of graphene [125–127]. For gas sensors made up of ceramic nanofibers, the composition and the nanofiber configuration are other important characteristics that can be controlled to improve the sensor performance.

Liu et al. [32] prepared polycrystalline CeO₂ nanofibers by combination of electrospinning and calcination. The average diameter of the nanofibers was measured as 376 ± 55 nm. They displayed good morphological and structural stability at high temperatures (800–1000°C) and showed reversible, sensitive, and reproducible response when used for real-time oxygen (O₂) and carbon monoxide (CO) monitoring at 800°C and 1000°C, respectively [32]. Tong et al. [49] prepared acetone sensors based on LnFeO₃ (Ln = La, Nd, and Sm) nanofibers produced by electrospinning and investigated the effect of lanthanide on acetone sensing properties of the nanofibers at different temperatures and acetone concentrations. The results indicated that the lanthanides significantly affected the sensing properties of LnFeO₃. When exposed to 100 ppm acetone at 140°C, the SmFeO₃ sensor exhibited the largest sensing response (Response = 9.98). The response and recovery times for the SmFeO₃ sensor were about 17 and 16 s, respectively [49]. Ma et al. [34] prepared hollow perovskite praseodymium ferrite (PrFeO₃) nanofibers via electrospinning followed by calcination. The samples had a large specific surface area (33.74 m² g⁻¹) with mesoporous characteristics. They showed good selectivity, long-time stability at 180°C, and high response value. While the response time of the sensor to 10 ppm acetone was about 4 s, the recovery time was measured as 4 s. [34]. Teli and Nadathur [48] prepared

reusable, reversible dye doped nanofibrous silica and silica/PVP, and silica/PMMA membranes by combination of sol-gel and electrospinning and demonstrated their use as an effective optical gas sensor. A durable, sensitive, reversible, and visually detectable response to HCl and NH₃ was observed when the silica composite NF membranes was doped with a pH sensitive dye Bromothymol blue. Eliminating the need for electronic instrumentation, the regeneration of the doped NF membranes' color under mild thermal treatment and their thermal stability, permitted their repeated use for naked-eye sensing. The magnitude of color change was affected by the presence of copolymer in the NF membrane structure due to the copolymer's effects on the fiber diameter, surface area, porosity, and polarity of nanofiber membranes. The reliable and reproducible visual sensor performance along with its flexible and porous nature offered many advantages for different applications such as detecting volatiles relevant to environmental safety, tracing stability to spoilage in fresh food storage, air quality monitoring. Besides, they could be used to detect biogenic amines, or volatiles released by biological materials, to monitor plant life or human health, and to confirm the safety of work environments in chemical and nuclear plants [48]. Han et al. [33] fabricated perovskite samarium ferrite (SmFeO₃) nanofibers by electrospinning route and calcination process for use as a sensor for ethylene glycol, which is on one hand one of the most significant raw materials, and on the other hand one of toxic pollutants for animals, humans, and environments. The roughness of SmFeO₃ nanofibers contributed to gas sensing properties by increasing the contact area between gases and material surface. They displayed high response value (18.19) to 100 ppm EG at 240°C, fast response/recovery times, good stability and selectivity [33].

3.3 Water remediation applications

Water resources being contaminated by many different types of pollutants such as heavy metal ions, organic dyes, pesticides, bacterial pathogens, etc. generates a major challenge worldwide. Many of these contaminants are skin sensitizers and mutagens responsible for different types of cancers in human beings. On the other hand, bacterial pathogens are responsible for several severe health problems. It has become very critical to develop efficient water purification technologies. Among many different methods such as electrochemical treatment, ozonation, membrane filtration, flocculation, ceramic nanofibers have gained significant interest because of their potential in water remediation due to their adsorption properties and photocatalytic activity. The major advantages of nanofibers in water remediation applications are their high aspect ratio, enhanced surface area, higher surface activity, higher porosity, continuous structure, easy handling and retrieving compared to nanoparticles [53].

Many attempts have been devoted to the use of ceramic nanofibers in the removal of contaminants from water sources. Fe₂O₃ [50], ZnO/TiO₂ [51], TiO₂ [52], CuO/ZnO [53], ZnO/SnO₂ [54], ZnO [55], NiO [83], and many other nanofibers have been developed and proved to be successful in water remediation applications.

Nalbandian et al. [50] produced α -Fe₂O₃ nanofibers via electrospinning and investigated their applicability in chromate removal from water. Adsorption capacity of the nanofibers increased as the average nanofiber diameter decreased. Based on (CrO₄²⁻) adsorption isotherms at pH 6, the nanofibers with 23 nm average diameter exhibited an adsorption capacity of 90.9 mg g⁻¹ [50]. Malval et al. [53] fabricated CuO-ZnO composite nanofibers and explored their adsorption capacity and antibacterial properties. The composite ceramic nanofibers displayed excellent adsorption capacity for congo red dye. Depending on the adsorption isotherms and kinetic studies composite nanofibers performed better than their single

counterparts. The ceramic nanofibers were also very active inhibitors against the growth of *S. aureus* and *GFP-E. Coli*. With their excellent adsorption capacity and adequate antibacterial properties, the composite ceramic nanofibers were suggested for use in water treatment and purification processes [53].

Nalbandian et al. [52] produced titanium dioxide (TiO₂) nanofibers and tailored their structure and composition to optimize their photocatalytic treatment efficiency. Nanofibers with controlled diameter (30–210 nm), crystal structure (anatase, rutile, mixed phases), and grain size (20–50 nm) were manufactured. Besides, composite nanofibers with either surface-deposited or bulk-integrated Au nanoparticle cocatalysts were developed. When the nanofibers' reactivity against some model pollutants such as phenol and emerging pollutants such as pharmaceuticals, personal care products were analyzed, optimized TiO₂ nanofibers displayed superior performance than the traditional nanoparticulate photocatalysts. The photoactivity increased by 5 to 10 fold after Au deposition onto the surface of the nanofibers independent of the solution concentration which was attributed to the improved charge separation [52]. Malval et al. [83] produced nickel oxide (NiO) nanofibers for use as photocatalysts. The NiO nanofibers were tested for their photoactivity against model dye congo red (CR). The concentration of the catalyst was observed to be a significant factor. Due to their non-aggregating nature in aqueous solution, NiO nanofibers performed better than NiO nanoparticles. Additionally, reusability and stability were other advantages NiO nanofibers provided [83]. Pascariu et al. [54] fabricated ZnO–SnO₂ nanofibers by electrospinning technique combined with calcination at 600°C. The composite ceramic nanofibers showed photocatalytic activity against Rhodamine B (RhB) dye and the highest efficiency was obtained for nanofibers with Sn/Zn molar ratio of 0.030 [54]. Pant et al. [55] produced fly ash incorporated zinc oxide nanofibers and investigated their ability to remove methylene blue (MB) from the water. Adding fly ash, which is a waste material from thermal power plants to ZnO nanofibers resulted in increased adsorption and photocatalytic removal of MB from water. Huh et al. [51] prepared TiO₂-coated yttria-stabilized zirconia/silica nanofiber (an) by coating TiO₂ on the surface of YSZ/silica NF using a sol–gel process. The coating layer improved the separation ability of the membrane as well as the photocatalytic degradation ability. With its smaller pore size, TiO₂-coated YSZ/silica NF membrane rejected over 99.6% of the 0.5 μm polymeric particles. Furthermore, the TiO₂-coated YSZ/silica NF membrane showed excellent adsorption/degradation of humic acid (HA, 88.2%), methylene blue (MB, 92.4%), and tetracycline (TC, 99.5%) [51].

Some polymer-ceramic composites have been suggested for the removal of organic pollutants from water. Allabashi et al. [56] impregnated Al₂O₃, SiC and TiO₂ ceramic nanofibers by triethoxysilylated derivatives of poly (propylene imine) dendrimer, polyethylene imine and polyglycerol hyperbranched polymers and β-cyclodextrin and subsequently sol–gel reaction led to their polymerization and chemical bond formation with the ceramic substrates. The resulting organic–inorganic filters were found to remove the polycyclic aromatic hydrocarbons (up to 99%), of monocyclic aromatic hydrocarbons (up to 93%), trihalogen methanes (up to 81%), pesticides (up to 43%) and methyl-tert-butyl ether (up to 46%) [56].

3.4 Batteries

Electrospun ceramic nanofibers, with their extremely high surface area and fast charge-transfer channels along its 1D nanostructure, have been considered as ideal materials for batteries. The use of lithium-ion batteries (LIBs) has attracted great interest for use in the smart micro-electronic devices and electric vehicles because of their potential for high energy density and power. However, their energy

density is usually restricted by the working potentials and specific capacity of the electrodes. There is great effort to develop alternative electrodes with higher specific capacity that will be able to replace commercially available graphite anode. Due to their high theoretical specific capacity, transition metal oxides have attracted considerable attention.

Recently, Zaidi et al. [57] prepared a separator film by electrospinning to develop high-performance LIBs. The film had a hybrid morphology of SiO₂ nanofibers (SNFs) and Al₂O₃ nanoparticles (ANPs). It had a polymer-free composition, smooth surface, good thermal stability with high electrolyte uptake (876%) and high porosity (79%). Compared to some commercial products, higher ionic conductivity, lower bulk resistance at elevated temperature (120°C), lower interfacial resistance with lithium metal, and a wider electrochemical window was obtained. When full cells were fabricated, the specific capacity of the full cell with the SNF-ANP separator film was measured as 165 mAh g⁻¹; the cell was stable for 100 charge/discharge cycles and exhibited a capacity retention of 99.9% at room temperature [57]. Jing et al. [59] used electrospun ZrO₂ membrane as separator in lithium or sodium batteries. The membranes displayed remarkable mechanical flexibility, excellent electrolyte wettability, and infiltration, ample porosity, high electrochemical inertness, and outstanding heat and flame-resistance. The separator could withstand high current densities and showed longer cycling life than the state-of-the-art separators [59].

Different types of CNFs were also developed as electrodes for batteries. Gangaja et al. [60] electrospun CuO nanofibers for use as LIB anode. The nanofibers were made up of CuO nanoparticles, which formed a good inter-connected network. Fabricated half cells maintained specific capacity of 310 mAh g⁻¹ at 1°C rate for 100 cycles and stabilized capacity of about 120 mAh g⁻¹ at 5°C rate for 1000 cycles. While SEI layer content remained the same, its thickness increased at the end of 10th charge according to the ex situ x-ray photoelectron spectroscopy [60].

Incorporation of carbon materials into ceramic nanofibers has been used as an effective strategy to improve electrical conductivity and act as a buffer to suppress the volume variation of the anodes. For example, addition of graphene into Co₃O₄ anodes has improved the electrochemical performance because of the high capacity of Co₃O₄ together with the high surface area, excellent flexibility of graphene, and good electrical conductivity [128, 129]. Hu et al. [61] synthesized porous Co₃O₄@rGO nanofiber anode materials via electrospinning, post thermal and hydrothermal treatments. The interconnected structure of Co₃O₄ nanocrystals and presence of reduced graphene oxide networks were effective in accommodating volume change, deterring aggregation of Co₃O₄ fibers and facilitating rapid Li⁺ ion transport during charge/discharge cycling. The developed anode material exhibited high reversible capacity, good rate capability, and excellent cycling stability when it was tested in half and full cells. The full cell constructed from a LiMn₂O₄ cathode and a Co₃O₄@rGO anode displayed a stable capacity with operation voltage of ~2.0 V, which was promising for the electronic devices working at low voltages [61].

CNFs with their high ionic conductivity are promising candidates for use as electrolytes in all-solid-state batteries, which are among the most promising technologies to replace conventional lithium-ion batteries [130]. Cui et al. [58] prepared an electrolyte using polyethylene oxide–lithium (bis trifluoromethyl) sulfate–succinonitrile (PLS) and frameworks of three-dimensional SiO₂ nanofibers (3D SiO₂ NFs), which had a conductivity of 9.32 × 10⁻⁵ S/cm at 30°C. While the Li/LiFePO₄ cells assembled with PLS and 3D SiO₂ NFs (PLS/3D SiO₂ NFs) delivered an original specific capacity of 167.9 mAh g⁻¹, they only suffered 3.28% capacity degradation after 100 cycles. The solid lithium batteries based on composite electrolytes offered high safety at elevated temperatures since the cells automatically shut down

with the decomposition of PLS above 400°C [58]. Yang et al. [62] developed a solid-state ceramic/polymer composite electrolyte by embedding a three-dimensional (3D) electrospun aluminum-doped $\text{Li}_{0.33}\text{La}_{0.557}\text{TiO}_3$ (LLTO) nanofiber network in a polyvinylidene fluoride-hexafluoropropylene (PVDF-HFP) matrix and reported an enhanced interfacial Li-ion transport along the nanofiber/polymer interface. The chemical interaction between the nanofibers and the polymer was further enhanced by coating lithium phosphate onto the LLTO nanofiber surface, which also promoted the lithium-ion transport along the polymer/nanofiber interface, improved the ionic conductivity and electrochemical cycling stability of the nanofiber/polymer composite. The full cell consisted of a lithium metal anode, a LiFePO_4 -based cathode and the composite electrolyte in between exhibited excellent cycling performance and rate capability [62]. Zhang et al. [63] embedded $\text{Li}_7\text{La}_3\text{Zr}_2\text{O}_{12}$ (LLZO) nanofibers into a poly(vinylidene fluoride-co-hexafluoropropylene) (PVDF-HFP)/ionic liquid (IL) matrix to construct a solid polymer electrolyte (SPE). The developed SPE, containing 15 wt. % LLZO nanofibers, exhibited an improved ionic conductivity ($6.5 \times 10^{-3} \text{ S cm}^{-1}$) at room temperature, a wide electrochemical window (5.3 V vs. Li/Li^+), excellent flexibility and mechanical strength. SPE-based half and full cells delivered impressive electrochemical properties [63].

3.5 Catalyst supports and catalysts

Ceramic nanofibers with their unique properties have been extensively explored as either catalyst supports or catalysts for various types of heterogeneous reactions, such as sinter-resistant catalysts [68], photocatalytic reaction [71], electrocatalytic reaction [69], hydrogenation reaction [70], oxidation reaction [66], and Suzuki coupling reactions [67].

Fu et al. [68] prepared $\gamma\text{-Al}_2\text{O}_3$ nanofibers with a loofah-like surface using single-needle electrospinning for use as Pt supports. After sintering at 500°C, the Al_2O_3 nanofiber supported Pt catalysts were employed in catalytic reduction of p-nitrophenol and 4-times higher reaction rate constant ($6.8 \text{ s}^{-1} \text{ mg}^{-1}$) was observed compared to Pt nanocrystals. The high performance of the Al_2O_3 nanofiber supported Pt catalysts was attributed to the special surface structure and the strong metal-support interactions between Pt and $\gamma\text{-Al}_2\text{O}_3$ [68]. There are many studies on the use of ceramic nanofibers as photocatalysts in water remediation studies, as already explained previously. Other than water remediation studies, ceramic nanofibers are also employed in the photocatalytic H_2 evolution from water splitting, which is a promising renewable energy generation process. Using electrospinning method, Wang et al. [71] fabricated MgTiO_3 nanofibers and compared their photocatalytic H_2 generation ability with the MgTiO_3 nanoparticles and P25. The MgTiO_3 nanofibers showed high efficiency and stability in photocatalytic H_2 generation under ultraviolet light. Attributed mainly to their large specific surface area, special 1D structure, unique mesh morphology, and pure phase, photoelectrochemical measurements showed that the MgTiO_3 nanofibers facilitated the transport and separation of the photoinduced charge carriers [71]. Ceramic nanofibers are also utilized in electrocatalysis to speed up the charge transfer reaction between electrodes and electrolytes. Hosseini et al. [69] fabricated CuO/NiO composite nanofibers and investigated their photocatalytic performance as anode catalyst for hydrazine oxidation in alkaline media. The best catalytic performance was observed when the proportion of $\text{Cu(OAc)}_2\text{:Ni(OAc)}_2$ was 25:75 in polymeric solution [69]. Liu et al. [70] electrospun mesoporous CeO_2 -based ultrathin nanofibers in fibril-in-tube configuration. The fibril-in-tube configuration was achieved by choosing two metal precursors with different decomposition rates. Al(acac)_3 , which rapidly led to the growth kinetics varied along the radial direction of nanofibers by releasing

gaseous pieces, was selected as Al_2O_3 precursor, and made critical contribution to the formation of fibril-in-tube structure. The novel fibril-in-tube CeO_2 nanofibers with different amount of homogenous Al_2O_3 elemental distribution were investigated as Pt supports. The developed catalytic system exhibited sinter-resistant catalytic activity in the hydrogenation of p-nitrophenol, which was 13-times higher than that of Pt@ Al_2O_3 catalyst [70]. Electrospun ceramic nanofibers are also employed as heterogeneous catalysts for oxidation reactions. Formo et al. [67] reported the use of TiO_2 and ZrO_2 nanofibers decorated with Pt, Pd, and Rh nanoparticles as a catalytic system for Suzuki cross-coupling reactions. The new catalytic system offered an efficient process, which was cost-effective as it could be fully regenerated and repeatedly used [67]. Formo et al. deposited Pt nanoparticles on the TiO_2 porous nonwoven mats, which acted as superior catalyst toward methanol oxidation reaction [66].

3.6 EMI shielding applications

Intensive effort is being spent to develop high-performance EMI shielding materials to protect people from the potential damages of high frequency electromagnetic waves generated by the electronic devices. Among many different electromagnetic wave absorbers such as carbon nanotubes, hollow carbon microspheres, graphene, Fe_3O_4 microspheres, composite spheres, needle-like metal oxides, and carbon nanofibers, specifically SiC nanofibers are considered as an important candidate because of their high temperature stability, mechanical strength, and resistance to oxidation and corrosion [75].

Wang et al. [75] fabricated flexible, hydrophobic, corrosion resistant, and thermally stable SiC ceramic nanofibers, which showed excellent EMI shielding properties with an effective absorption bandwidth of 4–18 GHz. 90% of electromagnetic waves below –10 dB were absorbed. The maximum reflection loss (RL) reached –19.4 dB at 5.84 GHz. Besides, they were found to be environmentally stable in 2 mol L^{-1} NaOH solution for 2 h and at high temperatures of 500°C in air atmosphere. The developed SiC nanofibers were suggested as candidates for EMI shielding materials in harsh environments [75]. In another study [76], they incorporated graphite into SiC/ Si_3N_4 composite nanofibers and investigated the relationship between processing, fiber microstructure, and their electromagnetic wave absorption performance. The annealing atmosphere and temperature were observed to affect the electromagnetic wave absorption capability and effective absorption bandwidth. The nanofibers after annealing at 1300°C in Ar showed a minimum RL of –57.8 dB at 14.6 GHz with EAB of 5.5 GHz. The nanofibers annealed at 1300°C in N_2 exhibited a minimum RL value of –32.3 dB at a thickness of 2.5 mm, and the EAB reached 6.4 GHz over the range of 11.3–17.7 GHz. The superior EMI shielding properties (high reflection loss together with wider EAB) imparted the composite nanofibers the potential to be used as reinforcements in polymer and ceramic matrix composites with EMI shielding properties [76]. Huo et al. [72] prepared heterogeneous SiC/ZrC/SiZrOC hybrid nanofibers with different ZrC contents and analyzed them in terms of electrical conductivity, average diameter, and microwave-absorbing capability. When the ZrC concentration increased from 0 to 10 wt.%, decrease in average nanofiber diameter from 800 nm to 200 nm and increase in electrical conductivity from 0.3448 to 2.5676 S cm^{-1} were observed. The minimum reflection loss was measured as –40.38 dB at 14.1 GHz for the SiC/ZrC/SiZrOC hybrid nanofibers and they were suggested as promising high temperature microwave-absorbing materials [72]. Using a combined process of electrospinning and calcination, Huo et al. [73] produced silicon carbide/carbon (SiC/C) hybrid nanofibers, which possessed a high aspect ratio and a scaly surface.

The EMI shielding properties of the SiC/C composite nanofibers were studied in the range from 2 GHz to 18 GHz. A paraffin matrix, which was reinforced with 30 wt. % composite nanofibers and had a thickness of 3 mm showed satisfactory dielectric loss value and a minimal reflection loss of approximately -36 dB at 6.8 GHz. Moreover, the maximum effective absorption (<-10 dB) bandwidth (EAB) was approximately 4.1 GHz (12.6–16.7 GHz) with a 1.5 mm thickness, which could cover most of the Ku-band [73]. Hou et al. [74] also fabricated flexible and lightweight ZrC/SiC hybrid nanofiber mats. When ZrC was added into SiC electrospinning solution, the viscosity decreased and the conductivity increased as a result of which the average diameter reduced from 2.6 μm to 330 nm, the specific BET surface area (SBET) increased from 51.5 to 131.1 $\text{m}^2 \text{g}^{-1}$ and the electrical conductivity increased from 1.5×10^{-6} to $1.3 \times 10^{-1} \text{ S cm}^{-1}$. It is found that 3-layer ZrC/SiC nanofiber mats with a thickness of 1.8 mm showed EMI shielding effectiveness (SET) of 18.9 dB, which could be further improved to 20.1 dB at 600°C [74].

3.7 Thermal insulation materials

Ceramic nanofibers exhibit excellent thermal stability and low thermal conductivity, which make them highly desirable for high-temperature thermal insulation applications [26]. Additionally, polymer phase used in electrospinning of ceramic nanofibers results in the formation of nanosized pores after calcination and helps to improve the insulation properties of ceramic nanofibers [131].

Si et al. [77] electrospun ultra-soft and strong silica nanofibers (SNF) from a sol-gel solution containing NaCl, the incorporation of which significantly enhanced the tensile strength of the SNF membranes from 3.2 to 5.5 MPa. The calcination temperature and the NaCl content in the precursor solution were found to affect the morphology and mechanical properties of the membranes. The membranes exhibited an ultra-softness of 40 mN, relative high tensile strength of 5.5 MPa and an ultra-low thermal conductivity of $0.0058 \text{ W m}^{-1} \text{ K}^{-1}$, which made them promising candidates for bunker clothing [77]. Dong et al. [79] fabricated fine-grained mullite nanofibers derived from the diphasic mullite sol (polymethyl siloxane and aluminum tri-sec-butoxide) by electrospinning and subsequent pyrolysis at 1500°C. Mullite fibers with 216 nm average diameter and ~ 100 nm grain size were obtained after sintering at 1500°C were suggested as high-temperature thermal insulation materials [79]. Si et al. [78] reported a scalable strategy to create superelastic lamellar-structured ceramic nanofibrous aerogels by combining SiO_2 nanofibers with aluminoborosilicate matrices. The developed nanofibrous aerogels exhibited the integrated properties of flyweight densities of $>0.15 \text{ mg cm}^{-3}$, zero Poisson's ratio, rapid recovery from 80% strain, and temperature-invariant superelasticity up to 1100°C, robust fire resistance and thermal insulation performance [78]. Dou et al. [81] designed a hierarchical cellular structured silica nanofibrous aerogel by using electrospun SiO_2 nanofibers (SNFs) and SiO_2 nanoparticle aerogels (SNAs) as the matrix and SiO_2 sol as the high-temperature analogue. They obtained randomly deposited SNFs with the SNAs evenly distributed on the fibrous cell wall. The unique hierarchical cellular structure of the ceramic nanofibrous aerogels exhibited ultralow density of $\sim 0.2 \text{ mg cm}^{-3}$, ultralow thermal conductivity ($23.27 \text{ mW m}^{-1} \text{ K}^{-1}$), negative Poisson's ratio, temperature-invariant superelasticity from -196 to 1100°C, and editable shapes on a large scale. The novel nanofibrous aerogels with their favorable properties were suggested as thermal insulation materials for aerospace, industrial, and even extreme environmental conditions [81]. Using electrospinning technique, Zhang et al. [26] prepared multi-phase SiZrOC nanofiber membranes composed of amorphous SiOC and ZrO_2 nanocrystals to solve the incompatibility between thermal stability and low thermal conductivity

of single-phase ceramic nanofibers at high temperatures, which limit their practical use. The fabricated SiZrOC nanofibers exhibited excellent high-temperature stability ($\sim 1200^\circ\text{C}$ in Ar) and low thermal conductivity ($\sim 0.1392 \text{ W m}^{-1} \text{ K}^{-1}$ at 1000°C in N_2). The unique combination of amorphous SiOC and ZrO_2 nanocrystals offered a novel strategy to produce high-performance thermal insulation materials. While the multi-phase interfaces and the ZrO_2 nanocrystals created thermal transfer barriers to reduce the heat transfer, the SiOC phase effectively suppressed radiative heat transfer [26]. Zhang et al. [82] produced ultra-strong, superelastic, and high temperature resistant, lamellar multiarc structured ceramic nanofibrous aerogels by combining $\text{ZrO}_2 - \text{Al}_2\text{O}_3$ nanofibers with $\text{Al}(\text{H}_2\text{PO}_4)_3$ matrices. The resulting $\text{ZrO}_2 - \text{Al}_2\text{O}_3$ nanofibrous aerogels displayed a recovery of 90%, compression strength of more than 1100 kPa, temperature-invariant superelasticity, and high fatigue resistance, thermal insulation performance with low thermal conductivity ($0.0322 \text{ W m}^{-1} \text{ K}^{-1}$), and temperature resistance up to 1300°C [82]. Peng et al. [80] fabricated yttria-stabilized zirconia mixed silica (YSZ/ SiO_2) nanofibers by the electrospinning method. The use temperature of the nanofibers increased by nearly 300°C and their maximum strength reached $5.9 \pm 0.8 \text{ MPa}$. The YSZ/ SiO_2 nanofibers, showing good thermal insulation performance and hydrophobic properties, were suggested for use as high-temperature insulation materials [80].

3.8 Other applications

CNFs have been intensely investigated and applied in many different applications since their first production in 2002. There is still an ever-growing interest in the field with emerging applications that influence different aspects of life.

Apart from the above discussed applications, ceramic nanofibers are also utilized in separation of nuclear waste and recycling of nuclear fuels. Liu et al. [84] electrospun TiO_2 nanofibers with high porosity and functionalized the membranes with silver nanoparticles and nanocrystal metal organic frameworks to capture gases of interest in order to recycle nuclear and industrial waste. These ceramic nanofiber materials showed high porosity, loading capacity, permeability, stability in extreme conditions and were effective in recycling of nuclear waste back into the fuel cycle [84].

Ramaseshan and Ramakrishna [85] produced zinc titanate ceramic nanofibers by electrospinning technology using polyvinylpyrrolidone as a binder for use as catalysts for the detoxification of chemical warfare agents, which are known to react with metal oxides (Mg, Al, Fe, Ti, Zn, Cr, Cu, Mn, etc.) and detoxify them into nontoxic harmless by-products. The zinc titanate nanofibers were found to be effective in decontamination of agents, such as dimethyl methyl phosphonate and chloroethyl ethyl sulfide. The extent of detoxification was measured and the products of reaction of zinc titanate against the simulants were found to be relatively harmless. The nanofibers obtained were suggested to replace conventional-activated carbon by electrospun ceramic nanofibers for face masks and protective clothing [85].

Abdo et al. [86] fabricated titanium dioxide (TiO_2) and carbon nanofibers by electrospinning technique followed by calcination process and utilized these nanofibers to reinforce magnesium matrix composites. When 5 wt.% TiO_2 nanofibers were added the ultimate compressive strength increased to 281 MPa, which was about 12.4% higher than the pure Mg. As a result of the addition of carbon nanofibers into magnesium matrix composites, hardness increased to 64.4% with slight sacrifice in the mechanical properties [86].

CNFs were also utilized in development of highly sensitive and reliable capacitive pressure sensors. Using flexible TiO_2 ceramic nanofibrous networks, Fu et al. [87] developed a capacitive pressure sensor and studied the capacitance-to-pressure

sensitivity. The ceramic pressure sensors, which exhibited high sensitivity ($\approx 4.4 \text{ k Pa}^{-1}$), fast response speed ($< 16 \text{ ms}$), ultralow limit of detection ($< 0.8 \text{ Pa}$), low fatigue over 50000 loading/unloading cycles, high temperature stability, were suggested for use as real-time health monitoring and motion detection [87].

4. Conclusions

The development of ceramic nanofibers has attracted a significant interest over the recent years. Among different production techniques such as magnetron sputtering, solution blowing, laser spinning, chemical vapor deposition, template synthesis, phase separation, hydrothermal treatment; electrospinning enabled the production of uniform CNFs with high surface areas, very small diameters, extremely long length, and small pore size. Ceramic nanofibers became indispensable materials in many applications. In this chapter, electrospun ceramic nanofibers are reviewed with an emphasis on their applications in tissue engineering, gas sensors, water remediation, batteries, catalyst supports/catalysts, electromagnetic interference shielding and thermal insulation materials. Although there has been a lot of progress since their first production, there is still a lot to be explored regarding their production, and properties, and there is a great potential for their uses in many different fields.

Funding

The author(s) received no financial support for the research, authorship, and/or publication of this article.

Conflict of interest


The author(s) declared no potential conflicts of interest with respect to the research, authorship, and/or publication of this article.

Author details

Nuray Kizildag
Integrated Manufacturing Technologies Research and Application Center,
Sabanci University, Istanbul, Turkey

*Address all correspondence to: nuray.kizildag@sabanciuniv.edu

IntechOpen

© 2021 The Author(s). Licensee IntechOpen. This chapter is distributed under the terms of the Creative Commons Attribution License (<http://creativecommons.org/licenses/by/3.0>), which permits unrestricted use, distribution, and reproduction in any medium, provided the original work is properly cited. 

References

- [1] Wang L, Yu Y, Chen PC, Zhang DW, Chen CH. Electrospinning synthesis of C/Fe₃O₄ composite nanofibers and their application for high performance lithium-ion batteries. *J Power Sources*. 2008;183(2):717-723.
- [2] Liu L, Lyu J, Mo J, Yan H, Xu L, Peng P, et al. Comprehensively-upgraded polymer electrolytes by multifunctional aramid nanofibers for stable all-solid-state Li-ion batteries. *Nano Energy*. 2020;69:104398.
- [3] Cho C-J, Chang Y-S, Lin Y-Z, Jiang D-H, Chen W-H, Lin W-Y, et al. Green electrospun nanofiber membranes filter prepared from novel biomass thermoplastic copolyester: Morphologies and filtration properties. *Journal of the Taiwan Institute of Chemical Engineers*. 2020;106:206-14.
- [4] Yu X, Li C, Tian H, Yuan L, Xiang A, Li J, et al. Hydrophobic cross-linked zein-based nanofibers with efficient air filtration and improved moisture stability. *Chem Eng J*. 2020;396:125373.
- [5] Kumar V, Mirzaei A, Bonyani M, Kim K-H, Kim HW, Kim SS. Advances in electrospun nanofiber fabrication for polyaniline (PANI)-based chemoresistive sensors for gaseous ammonia. *TrAC, Trends Anal Chem*. 2020;129:115938.
- [6] Li X, Chen S, Zhang X, Li J, Liu H, Han N, et al. Poly-l-Lactic Acid/Graphene Electrospun Composite Nanofibers for Wearable Sensors. *Energy Technology*. 2020;8(5):1901252.
- [7] Ito Y, Hasuda H, Kamitakahara M, Ohtsuki C, Tanihara M, Kang I-K, et al. A composite of hydroxyapatite with electrospun biodegradable nanofibers as a tissue engineering material. *Journal of Bioscience and Bioengineering*. 2005;100(1):43-9.
- [8] Lin W, Chen M, Qu T, Li J, Man Y. Three-dimensional electrospun nanofibrous scaffolds for bone tissue engineering. *Journal of Biomedical Materials Research Part B: Applied Biomaterials*. 2020;108(4):1311-21.
- [9] Khajavi R, Abbasipour M, Bahador A. Electrospun biodegradable nanofibers scaffolds for bone tissue engineering. *J Appl Polym Sci*. 2016;133(3).
- [10] Liu Y, Zhou S, Gao Y, Zhai Y. Electrospun nanofibers as a wound dressing for treating diabetic foot ulcer. *Asian Journal of Pharmaceutical Sciences*. 2019;14(2):130-43.
- [11] Bakhsheshi-Rad HR, Ismail AF, Aziz M, Akbari M, Hadisi Z, Omidi M, et al. Development of the PVA/CS nanofibers containing silk protein sericin as a wound dressing: In vitro and in vivo assessment. *Int J Biol Macromol*. 2020;149:513-21.
- [12] Sousa MGC, Maximiano MR, Costa RA, Rezende TMB, Franco OL. Nanofibers as drug-delivery systems for infection control in dentistry. *Expert Opinion on Drug Delivery*. 2020;17(7):919-30.
- [13] Celebioglu A, Uyar T. Electrospun formulation of acyclovir/cyclodextrin nanofibers for fast-dissolving antiviral drug delivery. *Materials Science and Engineering: C*. 2021;118:111514.
- [14] Daelemans L, Kizildag N, Van Paepegem W, D'Hooze DR, De Clerck K. Interdiffusing core-shell nanofiber interleaved composites for excellent Mode I and Mode II delamination resistance. *Compos Sci Technol*. 2019;175:143-50.
- [15] Daelemans L, Verschate O, Heirman L, Van Paepegem W, De Clerck K. Toughening mechanisms

- responsible for excellent crack resistance in thermoplastic nanofiber reinforced epoxies through in-situ optical and scanning electron microscopy. *Compos Sci Technol.* 2021;201:108504.
- [16] Barhoum A, Pal K, Rahier H, Uludb H, Kim I, Bechelany M. Nanofibers as new-generation materials: From spinning and nano-spinning fabrication techniques to emerging applications. *Applied Materials Today.* 2019;17:1-35.
- [17] Lupan O, Guérin VM, Ghimpu L, Tiginyanu IM, Pauporté T. Nanofibrous-like ZnO layers deposited by magnetron sputtering and their integration in dye-sensitized solar cells. *Chem Phys Lett.* 2012;550:125-9.
- [18] Huang Z, Kolbasov A, Yuan Y, Cheng M, Xu Y, Rojaee R, et al. Solution Blowing Synthesis of Li-Conductive Ceramic Nanofibers. *ACS Applied Materials & Interfaces.* 2020;12(14):16200-8.
- [19] Quintero F, Mann AB, Pou J, Lusquiños F, Riveiro A. Rapid production of ultralong amorphous ceramic nanofibers by laser spinning. *Appl Phys Lett.* 2007;90(15):153109.
- [20] Honda S-i, Baek Y-G, Ikuno T, Kohara H, Katayama M, Oura K, et al. SiC nanofibers grown by high power microwave plasma chemical vapor deposition. *Appl Surf Sci.* 2003;212-213:378-82.
- [21] Liu S, Shan H, Xia S, Yan J, Yu J, Ding B. Polymer Template Synthesis of Flexible SiO₂ Nanofibers to Upgrade Composite Electrolytes. *ACS Applied Materials & Interfaces.* 2020;12(28):31439-47.
- [22] Zhang Z-J, Zhao J, Qiao Z-J, Wang J-M, Sun S-H, Fu W-X, et al. Nonsolvent-induced phase separation-derived TiO₂ nanotube arrays/porous Ti electrode as high-energy-density anode for lithium-ion batteries. *Rare Metals.* 2020.
- [23] Chan JX, Wong JF, Hassan A, Shrivastava NK, Mohamad Z, Othman N. Green hydrothermal synthesis of high aspect ratio wollastonite nanofibers: Effects of reaction medium, temperature and time. *Ceram Int.* 2020;46(14):22624-34.
- [24] Wen Z, Song X, Chen D, Fan T, Liu Y, Cai Q. Electrospinning preparation and microstructure characterization of homogeneous diphasic mullite ceramic nanofibers. *Ceram Int.* 2020;46(8, Part B):12172-9.
- [25] Asadi-Pakdel K, Mehdivavaz Aghdam R, Shahedi Asl M, Faghihi Sani MA. Synthesis and morphology optimization of electrospun SiBNC nanofibers. *Ceram Int.* 2020;46(5):6052-9.
- [26] Zhang X, Wang B, Wu N, Han C, Wu C, Wang Y. Flexible and thermal-stable SiZrOC nanofiber membranes with low thermal conductivity at high-temperature. *J Eur Ceram Soc.* 2020;40(5):1877-85.
- [27] Kizildag N, Ucar N. Electrospinning Functional Polyacrylonitrile Nanofibers with Polyaniline, Carbon Nanotubes, and Silver Nitrate as Additives. In: Sajjad Haider, Haider A, editors. *Electrospinning - Material, Techniques, and Biomedical Applications:* IntechOpen; 2016. p. 25-43.
- [28] Kizildag N, Ucar N, Onen A, Karacan I. Polyacrylonitrile/polyaniline composite nano/microfiber webs produced by different dopants and solvents. *Journal of Industrial Textiles.* 2016;46(3):787-808.
- [29] Eren O, Ucar N, Onen A, Kizildag N, Karacan I. Synergistic effect of polyaniline, nanosilver, and carbon nanotube mixtures on the structure and properties of polyacrylonitrile

- composite nanofiber. *J Compos Mater.* 2016;50(15):2073-86.
- [30] Ucar N, Demirsoy N, Onen A, Karacan I, Kizildag N, Eren O, et al. The effect of reduction methods and stabilizer (PVP) on the properties of polyacrylonitrile (PAN) composite nanofibers in the presence of nanosilver. *Journal of Materials Science.* 2015;50(4):1855-64.
- [31] Pascariu P, Homocianu M. ZnO-based ceramic nanofibers: Preparation, properties and applications. *Ceram Int.* 2019;45(9):11158-73.
- [32] Liu Y, Ding Y, Zhang L, Gao P-X, Lei Y. CeO₂ nanofibers for in situ O₂ and CO sensing in harsh environments. *RSC Advances.* 2012;2(12):5193-8.
- [33] Han T, Ma SY, Xu XL, Xu XH, Pei ST, Tie Y, et al. Rough SmFeO₃ nanofibers as an optimization ethylene glycol gas sensor prepared by electrospinning. *Mater Lett.* 2020;268:127575.
- [34] Ma L, Ma SY, Shen XF, Wang TT, Jiang XH, Chen Q, et al. PrFeO₃ hollow nanofibers as a highly efficient gas sensor for acetone detection. *Sensors and Actuators B: Chemical.* 2018;255:2546-54.
- [35] Dai X, Shivkumar S. Electrospinning of hydroxyapatite fibrous mats. *Mater Lett.* 2007;61(13):2735-8.
- [36] Wu Y, Hench LL, Du J, Choy K-L, Guo J. Preparation of hydroxyapatite fibers by electrospinning technique. *J Am Ceram Soc.* 2004;87(10):1988-91.
- [37] Keskin S, Uslu İ, Tunç T, Öztürk M, Aytimur A. Preparation and characterization of neodymia doped PVA/Zr-Ce oxide nanocrystalline composites via electrospinning technique. *Mater Manuf Processes.* 2011;26(11):1346-51.
- [38] Starbova K, Petrov D, Starbov N, Lovchinov V. Synthesis of supported fibrous nanoceramics via electrospinning. *Ceram Int.* 2012;38(6):4645-51.
- [39] Zhang P, Jiao X, Chen D. Fabrication of electrospun Al₂O₃ fibers with CaO–SiO₂ additive. *Mater Lett.* 2013;91:23-6.
- [40] Shi Q, Vitchuli N, Nowak J, Caldwell JM, Breidt F, Bourham M, et al. Durable antibacterial Ag/polyacrylonitrile (Ag/PAN) hybrid nanofibers prepared by atmospheric plasma treatment and electrospinning. *Eur Polym J.* 2011;47(7):1402-9.
- [41] Reneker DH, Yarin AL. Electrospinning jets and polymer nanofibers. *Polymer.* 2008;49(10):2387-425.
- [42] Du Z, Zhou X, Ye P, Zeng X, Gan CL. Shape-memory actuation in aligned zirconia nanofibers for artificial muscle applications at elevated temperatures. *ACS Applied Nano Materials.* 2020;3(3):2156-66.
- [43] Franco PQ, João CFC, Silva JC, Borges JP. Electrospun hydroxyapatite fibers from a simple sol–gel system. *Mater Lett.* 2012;67(1):233-6.
- [44] Kim H-W, Kim H-E. Nanofiber generation of hydroxyapatite and fluor-hydroxyapatite bioceramics. *Journal of Biomedical Materials Research Part B: Applied Biomaterials.* 2006;77B(2):323-8.
- [45] Wang X, Gittens RA, Song R, Tannenbaum R, Olivares-Navarrete R, Schwartz Z, et al. Effects of structural properties of electrospun TiO₂ nanofiber meshes on their osteogenic potential. *Acta Biomaterialia.* 2012;8(2):878-85.
- [46] Aly IHM, Abed Alrahim Mohammed L, Al-Meer S, Elsaid K, Barakat NAM. Preparation and

characterization of wollastonite/titanium oxide nanofiber bioceramic composite as a future implant material. *Ceram Int.* 2016;42(10):11525-34.

[47] Nagarajan S, Belaid H, Pochat-Bohatier C, Teyssier C, Iatsunskyi I, Coy E, et al. Design of boron nitride/gelatin electrospun nanofibers for bone tissue engineering. *ACS Applied Materials & Interfaces.* 2017;9(39):33695-706.

[48] Teli MD, Nadathur GT. Reversible colourimetric sensing of volatile phase by dye doped electrospun silica based nanofibers. *Journal of Environmental Chemical Engineering.* 2020;8(4):103920.

[49] Tong Y, Zhang Y, Jiang B, He J, Zheng X, Liang Q. Effect of lanthanides on acetone sensing properties of LnFeO₃ nanofibers (Ln = La, Nd, and Sm). *IEEE Sens J.* 2017;17(8):2404-10.

[50] Nalbandian MJ, Zhang M, Sanchez J, Choa Y-H, Nam J, Cwiertny DM, et al. Synthesis and optimization of Fe₂O₃ nanofibers for chromate adsorption from contaminated water sources. *Chemosphere.* 2016;144:975-81.

[51] Huh JY, Lee J, Bukhari SZA, Ha J-H, Song I-H. Development of TiO₂-coated YSZ/silica nanofiber membranes with excellent photocatalytic degradation ability for water purification. *Scientific Reports.* 2020;10(1):17811.

[52] Nalbandian MJ, Greenstein KE, Shuai D, Zhang M, Choa Y-H, Parkin GF, et al. Tailored synthesis of photoactive TiO₂ nanofibers and Au/TiO₂ nanofiber composites: Structure and reactivity optimization for water treatment applications. *Environmental Science & Technology.* 2015;49(3):1654-63.

[53] Malwal D, Gopinath P. Efficient adsorption and antibacterial properties

of electrospun CuO-ZnO composite nanofibers for water remediation. *J Hazard Mater.* 2017;321:611-21.

[54] Pascariu P, Airinei A, Olaru N, Olaru L, Nica V. Photocatalytic degradation of Rhodamine B dye using ZnO-SnO₂ electrospun ceramic nanofibers. *Ceram Int.* 2016;42(6):6775-81.

[55] Pant B, Ojha GP, Kim H-Y, Park M, Park S-J. Fly-ash-incorporated electrospun zinc oxide nanofibers: Potential material for environmental remediation. *Environ Pollut.* 2019;245:163-72.

[56] Allabashi R, Arkas M, Hörmann G, Tsiourvas D. Removal of some organic pollutants in water employing ceramic membranes impregnated with cross-linked silylated dendritic and cyclodextrin polymers. *Water Res.* 2007;41(2):476-86.

[57] Zaidi SDA, Wang C, Shao Q, Gao J, Zhu S, Yuan H, et al. Polymer-free electrospun separator film comprising silica nanofibers and alumina nanoparticles for Li-ion full cell. *Journal of Energy Chemistry.* 2020;42:217-26.

[58] Cui J, Zhou Z, Jia M, Chen X, Shi C, Zhao N, et al. Solid polymer electrolytes with flexible framework of SiO₂ nanofibers for highly safe solid lithium batteries. *Polymers.* 2020;12(6):1324.

[59] Jing P, Liu M, Wang P, Yang J, Tang M, He C, et al. Flexible nonwoven ZrO₂ ceramic membrane as an electrochemically stable and flame-resistant separator for high-power rechargeable batteries. *Chem Eng J.* 2020;388:124259.

[60] Gangaja B, Chandrasekharan S, Vadukumpully S, Nair SV, Santhanagopalan D. Surface chemical analysis of CuO nanofiber composite

electrodes at different stages of lithiation/delithiation. *J Power Sources*. 2017;340:356-64.

[61] Hu R, Zhang H, Bu Y, Zhang H, Zhao B, Yang C. Porous Co_3O_4 nanofibers surface-modified by reduced graphene oxide as a durable, high-rate anode for lithium ion battery. *Electrochim Acta*. 2017;228:241-50.

[62] Yang H, Bright J, Chen B, Zheng P, Gao X, Liu B, et al. Chemical interaction and enhanced interfacial ion transport in a ceramic nanofiber-polymer composite electrolyte for all-solid-state lithium metal batteries. *Journal of Materials Chemistry A*. 2020;8(15):7261-72.

[63] Zhang W, Wang X, Zhang Q, Wang L, Xu Z, Li Y, et al. $\text{Li}_7\text{La}_3\text{Zr}_2\text{O}_{12}$ Ceramic nanofiber-incorporated solid polymer electrolytes for flexible lithium batteries. *ACS Applied Energy Materials*. 2020;3(6):5238-46.

[64] Dai Y, Chai Y, Sun Y, Fu W, Wang X, Gu Q, et al. New versatile Pt supports composed of graphene sheets decorated by Fe_2O_3 nanorods and N-dopants with high activity based on improved metal/support interactions. *Journal of Materials Chemistry A*. 2015;3(1):125-30.

[65] Dai Y, Formo E, Li H, Xue J, Xia Y. Surface-functionalized electrospun titania nanofibers for the scavenging and recycling of precious metal ions. *ChemSusChem*. 2016;9(20):2912-6.

[66] Formo E, Peng Z, Lee E, Lu X, Yang H, Xia Y. Direct oxidation of methanol on Pt nanostructures supported on electrospun nanofibers of anatase. *The Journal of Physical Chemistry C*. 2008;112(27):9970-5.

[67] Formo E, Yavuz MS, Lee EP, Lane L, Xia Y. Functionalization of electrospun ceramic nanofiber membranes with noble-metal nanostructures for

catalytic applications. *J Mater Chem*. 2009;19(23):3878-82.

[68] Fu W, Dai Y, Li JPH, Liu Z, Yang Y, Sun Y, et al. Unusual hollow Al_2O_3 nanofibers with loofah-like skins: Intriguing catalyst supports for thermal stabilization of Pt nanocrystals. *ACS Applied Materials & Interfaces*. 2017;9(25):21258-66.

[69] Hosseini SR, Ghasemi S, Kamali-Rousta M. Preparation of CuO/NiO composite nanofibers by electrospinning and their application for electro-catalytic oxidation of hydrazine. *J Power Sources*. 2017;343:467-76.

[70] Liu S, Tian J, Yin K, Li Z, Meng X, Zhu M, et al. Constructing fibril-in-tube structures in ultrathin CeO_2 -based nanofibers as the ideal support for stabilizing Pt nanoparticles. *Materials Today Chemistry*. 2020;17:100333.

[71] Wang L, Yang G, Peng S, Wang J, Ji D, Yan W, et al. Fabrication of MgTiO_3 nanofibers by electrospinning and their photocatalytic water splitting activity. *Int J Hydrogen Energy*. 2017;42(41):25882-90.

[72] Huo Y, Zhao K, Miao P, Kong J, Xu Z, Wang K, et al. Microwave absorption performance of $\text{SiC}/\text{ZrC}/\text{SiZrOC}$ hybrid nanofibers with enhanced high-temperature oxidation resistance. *ACS Sustainable Chemistry & Engineering*. 2020;8(28):10490-501.

[73] Huo Y, Zhao K, Xu Z, Tang Y. Electrospinning synthesis of SiC/Carbon hybrid nanofibers with satisfactory electromagnetic wave absorption performance. *J Alloys Compd*. 2020;815:152458.

[74] Hou Y, Cheng L, Zhang Y, Du X, Zhao Y, Yang Z. High temperature electromagnetic interference shielding of lightweight and flexible ZrC/SiC nanofiber mats. *Chem Eng J*. 2021;404:126521.

- [75] Wang P, Cheng L, Zhang Y, Wu H, Hou Y, Yuan W, et al. Flexible, hydrophobic SiC ceramic nanofibers used as high frequency electromagnetic wave absorbers. *Ceram Int.* 2017;43(10):7424-35.
- [76] Wang P, Cheng L, Zhang Y, Zhang L. Flexible SiC/Si₃N₄ composite nanofibers with in situ embedded graphite for highly efficient electromagnetic wave absorption. *ACS Applied Materials & Interfaces.* 2017;9(34):28844-58.
- [77] Si Y, Mao X, Zheng H, Yu J, Ding B. Silica nanofibrous membranes with ultra-softness and enhanced tensile strength for thermal insulation. *RSC Advances.* 2015;5(8):6027-32.
- [78] Si Y, Wang X, Dou L, Yu J, Ding B. Ultralight and fire-resistant ceramic nanofibrous aerogels with temperature-invariant superelasticity. *Science Advances.* 2018;4(4):eaas8925.
- [79] Dong X, Liu J, Li X, Zhang X, Xue Y, Liu J, et al. Electrospun mullite nanofibers derived from diphasic mullite sol. *J Am Ceram Soc.* 2017;100(8):3425-33.
- [80] Peng Y, Xie Y, Wang L, Liu L, Zhu S, Ma D, et al. High-temperature flexible, strength and hydrophobic YSZ/SiO₂ nanofibrous membranes with excellent thermal insulation. *J Eur Ceram Soc.* 2020.
- [81] Dou L, Zhang X, Cheng X, Ma Z, Wang X, Si Y, et al. Hierarchical cellular structured ceramic nanofibrous aerogels with temperature-invariant superelasticity for thermal insulation. *ACS Appl Mater Interfaces.* 2019;11(32):29056-64.
- [82] Zhang X, Wang F, Dou L, Cheng X, Si Y, Yu J, et al. Ultrastrong, superelastic, and lamellar multiarch structured ZrO₂-Al₂O₃ nanofibrous aerogels with high-temperature resistance over 1300 °C. *ACS Nano.* 2020.
- [83] Malwal D, Gopinath P. Fabrication and characterization of poly(ethylene oxide) templated nickel oxide nanofibers for dye degradation. *Environmental Science: Nano.* 2015;2(1):78-85.
- [84] Liu H, Bell N, Cipiti BB, Lewis TG, Sava DF, Nenoff TM. Functionalized ultra-porous titania nanofiber membranes as nuclear waste separation and sequestration scaffolds for nuclear fuels recycle. Albuquerque, New Mexico: Sandia National Laboratories; 2012. Report No.: SAND2012-8025.
- [85] Ramaseshan R, Ramakrishna S. Zinc titanate nanofibers for the detoxification of chemical warfare simulants. *J Am Ceram Soc.* 2007;90(6):1836-42.
- [86] Abdo HS, Khalil KA, El-Rayes MM, Marzouk WW, Hashem A-FM, Abdel-Jaber GT. Ceramic nanofibers versus carbon nanofibers as a reinforcement for magnesium metal matrix to improve the mechanical properties. *Journal of King Saud University - Engineering Sciences.* 2020;32(5):346-50.
- [87] Fu M, Zhang J, Jin Y, Zhao Y, Huang S, Guo CF. A highly sensitive, reliable, and high-temperature-resistant flexible pressure sensor based on ceramic nanofibers. *Advanced Science.* 2020;7(17):2000258.
- [88] Zhang J, Lu H, Lu H, Li G, Gao J, Yang Z, et al. Porous bimetallic Mo-W oxide nanofibers fabricated by electrospinning with enhanced acetone sensing performances. *J Alloys Compd.* 2019;779:531-42.
- [89] Wu J, Xing X, Zhu Z, Zheng L, Chen J, Wang C, et al. Electrospun hollow CuO modified V₂O₅ nano-string of pearls with improved acetone sensitivity. *Chem Phys Lett.* 2019;727:19-24.

- [90] Jeong YJ, Koo W-T, Jang J-S, Kim D-H, Kim M-H, Kim I-D. Nanoscale PtO₂ catalysts-loaded SnO₂ multichannel nanofibers toward highly sensitive acetone sensor. *ACS Applied Materials & Interfaces*. 2018;10(2):2016-25.
- [91] Cheng Y, He Y, Li S, Wang Y, Zhao Y, Li Y, et al. Ultra-sensitive and selective acetone gas sensor with fast response at low temperature based on Cu-doped α -Fe₂O₃ porous nanotubes. *Journal of Materials Science: Materials in Electronics*. 2018;29(13):11178-86.
- [92] Jeong YJ, Koo W-T, Jang J-S, Kim D-H, Cho H-J, Kim I-D. Chitosan-templated Pt nanocatalyst loaded mesoporous SnO₂ nanofibers: a superior chemiresistor toward acetone molecules. *Nanoscale*. 2018;10(28):13713-21.
- [93] Kou X, Xie N, Chen F, Wang T, Guo L, Wang C, et al. Superior acetone gas sensor based on electrospun SnO₂ nanofibers by Rh doping. *Sensors and Actuators B: Chemical*. 2018;256:861-9.
- [94] Yang HM, Ma SY, Yang GJ, Chen Q, Zeng QZ, Ge Q, et al. Synthesis of La₂O₃ doped Zn₂SnO₄ hollow fibers by electrospinning method and application in detecting of acetone. *Appl Surf Sci*. 2017;425:585-93.
- [95] Jiang Z, Yin M, Wang C. Facile synthesis of Ca²⁺/Au co-doped SnO₂ nanofibers and their application in acetone sensor. *Mater Lett*. 2017;194:209-12.
- [96] Zhang J, Lu H, Yan C, Yang Z, Zhu G, Gao J, et al. Fabrication of conductive graphene oxide-WO₃ composite nanofibers by electrospinning and their enhanced acetone gas sensing properties. *Sensors and Actuators B: Chemical*. 2018;264:128-38.
- [97] Koo W-T, Jang J-S, Choi S-J, Cho H-J, Kim I-D. Metal-organic framework templated catalysts: Dual sensitization of PdO-ZnO composite on hollow SnO₂ nanotubes for selective acetone sensors. *ACS Applied Materials & Interfaces*. 2017;9(21):18069-77.
- [98] Pascali CD, Signore MA, Taurino A, Francioso L, Macagnano A, Avossa J, et al. Investigation of the gas-sensing performance of electrospun TiO₂ nanofiber-based sensors for ethanol sensing. *IEEE Sens J*. 2018;18(18):7365-74.
- [99] Li F, Gao X, Wang R, Zhang T. Design of WO₃-SnO₂ core-shell nanofibers and their enhanced gas sensing performance based on different work function. *Appl Surf Sci*. 2018;442:30-7.
- [100] Chen D, Yi J. One-pot electrospinning and gas-sensing properties of LaMnO₃ perovskite/SnO₂ heterojunction nanofibers. *J Nanopart Res*. 2018;20(3):65.
- [101] Huang B, Zhang Z, Zhao C, Cairang L, Bai J, Zhang Y, et al. Enhanced gas-sensing performance of ZnO@In₂O₃ core@shell nanofibers prepared by coaxial electrospinning. *Sensors and Actuators B: Chemical*. 2018;255:2248-57.
- [102] Gao X, Li F, Wang R, Zhang T. A formaldehyde sensor: Significant role of p-n heterojunction in gas-sensitive core-shell nanofibers. *Sensors and Actuators B: Chemical*. 2018;258:1230-41.
- [103] Andre RS, Kwak D, Dong Q, Zhong W, Correa DS, Mattoso LHC, et al. Sensitive and selective NH₃ monitoring at room temperature using ZnO ceramic nanofibers decorated with poly(styrene sulfonate). *Sensors (Basel)*. 2018;18(4):1058.
- [104] Pang Z, Nie Q, Lv P, Yu J, Huang F, Wei Q. Design of flexible PANI-coated CuO-TiO₂-SiO₂ heterostructure nanofibers with high ammonia sensing

response values. *Nanotechnology*. 2017;28(22):225501.

[105] Pang Z, Nie Q, Wei A, Yang J, Huang F, Wei Q. Effect of In₂O₃ nanofiber structure on the ammonia sensing performances of In₂O₃/PANI composite nanofibers. *Journal of Materials Science*. 2017;52(2):686-95.

[106] Sankar Ganesh R, Durgadevi E, Navaneethan M, Patil VL, Ponnusamy S, Muthamizhchelvan C, et al. Low temperature ammonia gas sensor based on Mn-doped ZnO nanoparticle decorated microspheres. *J Alloys Compd*. 2017;721:182-90.

[107] Das M, Sarkar D. One-pot synthesis of zinc oxide - polyaniline nanocomposite for fabrication of efficient room temperature ammonia gas sensor. *Ceram Int*. 2017;43(14):11123-31.

[108] Xu L, Dong B, Wang Y, Bai X, Chen J, Liu Q, et al. Porous In₂O₃:RE (RE = Gd, Tb, Dy, Ho, Er, Tm, Yb) Nanotubes: Electrospinning Preparation and Room Gas-Sensing Properties. *The Journal of Physical Chemistry C*. 2010;114(19):9089-95.

[109] Bai S, Fu H, Zhao Y, Tian K, Luo R, Li D, et al. On the construction of hollow nanofibers of ZnO-SnO₂ heterojunctions to enhance the NO₂ sensing properties. *Sensors and Actuators B: Chemical*. 2018;266:692-702.

[110] Jaroenapibal P, Boonma P, Saksilaporn N, Horprathum M, Amornkitbamrung V, Triroj N. Improved NO₂ sensing performance of electrospun WO₃ nanofibers with silver doping. *Sensors and Actuators B: Chemical*. 2018;255:1831-40.

[111] Ponnuvelu DV, Abdulla S, Pullithadathil B. Novel Electro-Spun Nanograined ZnO/Au Heterojunction Nanofibers and Their Ultrasensitive

NO₂ Gas Sensing Properties. *ChemistrySelect*. 2018;3(25):7156-63.

[112] Wang C, Ma S, Sun A, Qin R, Yang F, Li X, et al. Characterization of electrospun Pr-doped ZnO nanostructure for acetic acid sensor. *Sensors and Actuators B: Chemical*. 2014;193:326-33.

[113] Katoch A, Sun G-J, Choi S-W, Byun J-H, Kim SS. Competitive influence of grain size and crystallinity on gas sensing performances of ZnO nanofibers. *Sensors and Actuators B: Chemical*. 2013;185:411-6.

[114] Wei S, Yu Y, Zhou M. CO gas sensing of Pd-doped ZnO nanofibers synthesized by electrospinning method. *Mater Lett*. 2010;64(21):2284-6.

[115] Galstyan V, Comini E, Baratto C, Faglia G, Sberveglieri G. Nanostructured ZnO chemical gas sensors. *Ceram Int*. 2015;41(10, Part B):14239-44.

[116] Koo W-T, Choi S-J, Kim S-J, Jang J-S, Tuller HL, Kim I-D. Heterogeneous sensitization of metal-organic framework driven metal@metal oxide complex catalysts on an oxide nanofiber scaffold toward superior gas sensors. *J Am Chem Soc*. 2016;138(40):13431-7.

[117] Li W, Ma S, Li Y, Yang G, Mao Y, Luo J, et al. Enhanced ethanol sensing performance of hollow ZnO-SnO₂ core-shell nanofibers. *Sensors and Actuators B: Chemical*. 2015;211:392-402.

[118] Lee C-S, Kim I-D, Lee J-H. Selective and sensitive detection of trimethylamine using ZnO-In₂O₃ composite nanofibers. *Sensors and Actuators B: Chemical*. 2013;181:463-70.

[119] Deng J, Yu B, Lou Z, Wang L, Wang R, Zhang T. Facile synthesis and enhanced ethanol sensing

- properties of the brush-like ZnO–TiO₂ heterojunctions nanofibers. *Sensors and Actuators B: Chemical*. 2013;184:21-6.
- [120] Lou Z, Deng J, Wang L, Wang R, Fei T, Zhang T. A class of hierarchical nanostructures: ZnO surface-functionalized TiO₂ with enhanced sensing properties. *RSC Advances*. 2013;3(9):3131-6.
- [121] Wan GX, Ma SY, Li XB, Li FM, Bian HQ, Zhang LP, et al. Synthesis and acetone sensing properties of Ce-doped ZnO nanofibers. *Mater Lett*. 2014;114:103-6.
- [122] Tang W, Wang J, Yao P, Li X. Hollow hierarchical SnO₂-ZnO composite nanofibers with heterostructure based on electrospinning method for detecting methanol. *Sensors and Actuators B: Chemical*. 2014;192:543-9.
- [123] Katoch A, Choi S-W, Sun G-J, Kim HW, Kim SS. Mechanism and prominent enhancement of sensing ability to reducing gases in p/n core-shell nanofiber. *Nanotechnology*. 2014;25(17):175501.
- [124] Song X, Wang Z, Liu Y, Wang C, Li L. A highly sensitive ethanol sensor based on mesoporous ZnO–SnO₂ nanofibers. *Nanotechnology*. 2009;20(7):075501.
- [125] Sun Ye, Zhang D, Chang H, Zhang Y. Fabrication of palladium–zinc oxide–reduced graphene oxide hybrid for hydrogen gas detection at low working temperature. *Journal of Materials Science: Materials in Electronics*. 2017;28(2):1667-73.
- [126] Kim D-H, Jang J-S, Koo W-T, Kim ID. Graphene oxide templating: facile synthesis of morphology engineered crumpled SnO₂ nanofibers for superior chemiresistors. *Journal of Materials Chemistry A*. 2018;6(28):13825-34.
- [127] Abideen ZU, Katoch A, Kim J-H, Kwon YJ, Kim HW, Kim SS. Excellent gas detection of ZnO nanofibers by loading with reduced graphene oxide nanosheets. *Sensors and Actuators B: Chemical*. 2015;221:1499-507.
- [128] Li B, Cao H, Shao J, Li G, Qu M, Yin G. Co₃O₄@graphene composites as anode materials for high-performance lithium ion batteries. *Inorg Chem*. 2011;50(5):1628-32.
- [129] Song MJ, Kim IT, Kim YB, Shin MW. Self-standing, binder-free electrospun Co₃O₄/carbon nanofiber composites for non-aqueous Li-air batteries. *Electrochim Acta*. 2015;182:289-96.
- [130] La Monaca A, Paoletta A, Guerfi A, Rosei F, Zaghbi K. Electrospun ceramic nanofibers as 1D solid electrolytes for lithium batteries. *Electrochem Commun*. 2019;104:106483.
- [131] Panda PK. Ceramic Nanofibers by Electrospinning Technique—A Review. *Transactions of the Indian Ceramic Society*. 2007;66(2):65-76.